ORIGINAL ARTICLE

Semaphorin3A promotes osseointegration of titanium implants in osteoporotic rabbits

An Song[1,2,3] · Feng Jiang[1,2,3] · Yi Wang[1,2,3] · Ming Wang[4] · Yanhui Wu[4] · Yang Zheng[1,2,3] · Xiaomeng Song[1,2,3] · Wei Zhang[2,3] · Junbo Zhou[4]

Abstract

Objective In the present study, we intend to assess the function of Sema3A in osseointegration of titanium implants both *in vivo* and *in vitro*.

Material and methods Briefly, Sema3A was transfected in HBMSCs cells to detect its effect on osteogenesis. Subsequently, an in vivo rabbit model was established. Eighteen female rabbits were randomly assigned into three groups (*n*=6), and rabbits in the two treatment groups (OVX groups) were subjected to bilateral ovariectomy, while those in the control group were treated with sham operation. Twelve weeks later, we first examined expression levels of Sema3A in rabbits of the three groups. Titanium implants were implanted in rabbit proximal tibia. Specifically, rabbits in sham group were implanted with Matrigel, while the remaining in the OVX experimental group (OVX+Sema3A group) and OVX group were implanted with Matrigel containing Sema3A adeno-associated virus or empty vector, respectively.

Results Histomorphometry results uncovered that rabbits in the OVX+Sema3A group had a significantly higher BIC compared with those of the OVX group on the 12th week of post-implantation. And compared with the OVX group, the maximum push-out force increased by 89.4%, and the stiffness increased by 39.4%, the toughness increased by 63.8% in the OVX+Sema3A group at 12 weeks.

Conclusion Sema3A has a positive effect on promoting early osseointegration of titanium implants in osteoporotic rabbits.

Clinical relevance Our research found that Sema3A can improve the osteogenic ability of bone marrow stem cells and promotes osseointegration during osteoporosis.

Keywords Bone-implant contact ratio · Implant osseointegration · NF-kappa B · Osteoporosis · Semaphorin3A

An Song and Feng Jiang contributed equally to this work.

✉ Wei Zhang
sxm813121@163.com

✉ Junbo Zhou
songan04551@163.com

1   Department of Oral and Maxillofacial Surgery, The Affiliated Stomatological Hospital of Nanjing Medical University, Nanjing, Jiangsu, People's Republic of China

2   Jiangsu Province Key Laboratory of Oral Diseases, Jiangsu Province and Stomatological Institute of Nanjing Medical University, No.1, Shanghai Road, Gulou District, Nanjing 210029, Jiangsu, People's Republic of China

3   Jiangsu Province Engineering Research Center of Stomatological Translational Medicine, Nanjing, China

4   Department of Stomatology, Nanjing Integrated Traditional Chinese and Western Medicine Hospital, No.179, Xiaolingwei Road, Xuanwu District, Nanjing 210014, Jiangsu, China

Introduction

In recent decades, implant supported prosthesis have been widely used to replace missing teeth [1]. However, the deficiency of bone quantity and quality can cause adverse effects on possibly implant supported prosthesis [2]. Traditionally, bone quantity deficiency can be improved by autogenous bone graft, allogeneic or xenogeneic bone transplantation, bone replacement, distraction osteogenesis, and many other methods [3, 4]. These methods, however, are not as enough to completely reverse the deficient bone quality [5]. It is reported that osteoporosis influences the alveolar process and impairs alveolar bone healing. Osteoporosis has become a major cause of fixation failure due to poor implant osseointegration and has an adverse effect on osseointegration of the dental implant [6]. Besides, osteoporosis also impairs the osseointegration and long-term stability of the implant [7]. Therefore, osteoporosis is as one of the recognized risks of dental implant treatment. Although the function of osteoporosis in implant osseointegration has been widely studied, the conclusions remain inconsistent [8].

Recently, bone tissue engineering and gene therapy have been highlighted because of their potentials in promoting bone regeneration [9]. These methods intend to generate new bone tissues in the bone defect area fast and efficiently as original bones [10]. Currently, several gene modification techniques have been used to promote osteogenesis and osseointegration around implants, including SATB2 and BMP-2, and they can promote osteoblasts [11]. It is necessary to develop a novel method that promotes the activity of osteoblasts, thus accelerating osteogenesis.

Semaphorin3A (Sema3A) is a member of the semaphorin family, which is of significance in the development of the nervous system, vascular system, immune system, and various other organs [12, 13]. Sema3A is the only secreted semaphorin protein, which exerts the biological function by binding to neurobilin1 (Nrp1)—PlexinA1 protein complex on the cell membrane surface [14]. Recently, Sema3A has been identified to inhibit osteoclast-induced bone resorption and accelerate osteoblast-induced bone formation, thus protecting bone metabolism. Besides, the use of Sema3A is capable of promoting bone deposition and repairing the wounded area of cortical bone defect in mice formed by artificial drilling. It is reported that an inhibition of osteoclasts induced by receptor activator of NF-kappa B ligand (RANKL) can cause bone resorption decline [16]. Interestingly, NF-kappa B promotes proliferative ability of osteoprogenitors and suppress differentiation of terminal osteoblasts [17]. The NF-kappa B signaling pathway is able to negatively control bone formation and activation of NF-kappa B significantly downregulates the key osteogenic transcription factor RUNX2 [18].

Sema3A plays an important role in accelerating osteogenesis. However, in vivo effect of Sema3A on osseointegration of implants is unclear. Therefore, in this study, we established a rabbit osteoporosis model and wanted to investigate the biological effect of Sema3A on implant osseointegration.

Methods

Cell culture and reagents

HBMSCs obtained from the American Type Culture Collection (ATCC, Manassas, VA, USA) were cultured in Dulbecco's modified Eagle's medium (DMEM) supplemented with 15% FBS and 1% penicillin/streptomycin at 37°C in 5% CO_2 atmosphere. Cells passaged to 3–6 generations were used in the experiments. Fresh medium was replaced with a 3-day interval. The full-length coding region of Sema3A was constructed by GenePharma (Shanghai, China); the recombinant adeno-associated virus vector overexpressing rabbit Sema3A and empty vector control were constructed by GenePharma (Shanghai, China). The sequences were as follows:si-Sema3A-1: 5′- GCUAGAAUAGGUCAGAUAUTT-3′; si-Sema3A-2:5′-GGAUGGACCCAACUAUCAATT-3′;si-Sema3A-3:5′-GCAAUGGAGCUUUCCACUATT-3′;si-NC: 5′-TTCTCCGAACGTGTCACGT-3′. Cells were cultured in a 6-well dish with 50–60% confluency, starved in medium without FBS for 16h and then transfections of HBMSCs cells with the related plasmids were performed with Lipofectamine 2000 (Invitrogen) according to the manufacturer's instructions. To induce stable transfection, transfected cells were selected with puromycin (2μg/mL)(Gibco).

Determination of alkaline and mineralized matrix formation

Cells were induced to osteogenic differentiation in the osteogenic medium containing 10mM β-glycerophosphate, 100nM dexamethasone (Sigma-Aldrich, St. Louis, MO, USA) and 100nM ascorbic acid for 14–21 days. ALP activity was quantified using an Alkaline Phosphatase Assay Kit (Jiancheng Corp., Nanjing, China). The formation of mineralized matrix nodules was determined by Alizarin Red S (pH=4.4) (Sigma-Aldrich) staining [19].

Real-time quantitative-polymerase chain reaction

Total RNA was isolated using TRIzol reagent (Vazyme Biotech, Nanjing, China). cDNA was synthesized using 5×PrimeScript RT Master Mix (Vazyme Biotech, Nanjing, China). QRT-PCR was performed using the SYBR Premix Ex Taq Kit (Vazyme Biotech, Nanjing, China) and ABI 7900 real-time PCR system (Applied Biosystems, 3175 Staley Road, Grand Island, NY). Relative levels were calculated by $2^{-\Delta\Delta CT}$ method and normalized to that of GAPDH. The primers were listed as follows:

Sema3A (5′→3′): CCCGAGACCCTTACTGTGCTT (forward), and TTGTCGTCTTGTGCGTCTCTTTG (reverse); ALP (5′→3′): TGGAGGTTCAGAAGCTCAAC ACCA (forward), and ATCTCGTTCTCTGAGTACCA GTC (reverse); OCN (5′→3′): CATGAGAGCCCTCACA (forward), and AGAGCGACACCCTAGAC (reverse); OPN (5′→3′): ATGGCCGAGGTGATAGTGTGG (forward), and CATCAGGGTACTGGATGTCAGGT (reverse); p65 (5′→3′): GTCCTTTCAGCGGACCCA (forward), and ACAGCAATGCGTCGAGGTG (reverse); IKBα(5′→3′): GGAAGTGATCCGCCAGGTGA (forward), and AGTGGAGTGGAGTCTGCTGC (reverse); GAPDH (5′→3′): GAAGGTGAAGGTCGGAGTC (forward), and GAGATGGTGATGGGATTTC (reverse).

Western blotting

After washing in pre-cooled PBS, cells were lysed in lysis buffer (Beyotime, Shanghai, China) for 30min. Isolated protein samples were fractionated by sodium dodecyl sulfate-polyacrylamide gel electrophoresis (SDS-PAGE) and then transferred to polyvinylidene difluoride (PVDF) membranes (Millipore, MA). The membranes were blocked using 5% BSA for 2h at room temperature (RT). Immunoblots were probed using primary antibodies overnight at 4°C, and washed in TBST (3×5min). Later, they were probed with horseradish peroxidase-conjugated (HRP) secondary antibodies (Proteintech Group, Wuhan, China) for 1h at RT. Finally, immunoreactive bands were exposed by an Immobilon Western Chemiluminescent HRP Substrate (Millipore) using the ImageQuantLAS 4000 mini imaging system (General Electrics). The blots were probed using primary antibodies and incubated overnight at 4°C: Sema3A (ab23393, abcam), ALP (ab229126, abcam), OPN (22952-1-AP, Proteintech), OCN (23418-1-AP, Proteintech), NF-kappa B p65 (#8242, CST), Phospho-NF-kappa B p65 (Ser536)(#3033, CST), IκBα(#4814S, CST), Phospho-IκBα (#5209S, CST), GAPDH (#5174S, CST).

Implants

The implant was designed using pure titanium with the following parameters: diameter = 2.5mm; length = 10mm; thread depth = 0.5mm; pitch thread = 1.2mm. The conical implants were manufactured by OSSTEM Co., Ltd. The surface of the implant was originally smooth. Implants were ultrasonically washed in deionized water, anhydrous ethanol, and deionized water in sequence (15 min each) and dried at RT. Sterilization of implants were conducted by 121°C autoclaving for 20 min.

Experimental rabbits

This study was approved by the Animal Care Committee of Nanjing First Hospital, Nanjing Medical University (IACUC Approval No. SYXK20160006). All animal procedures were in accordance with the Guidelines of International Standards on the Animal Ethical and Welfare Committee (AEWC), and the ARRIVE guideline for the care and use of laboratory animals released by National Institutes of Health (NIH Publications No. 8023, revised in 1978). A total of 18 New Zealand white female rabbits with 8 months old, weighing about 2.5–4.0kg were used in this experiment. Rabbits were housed in cages in a 12-h light/dark cycle and normally fed with free accesses to food and water. After 1 week of acclimatization, they were randomly assigned into three groups (n=6). Rabbits in two groups underwent ovariectomy surgery (OVX), while those in the control group had sham surgery (Supplemental Figure.1). After surgery, all rabbits were observed for 3 months. BMD was measured using a dual-energy X-ray absorptiometry (Lunar DPX-IQ, Lunar Co., Wisconsin, WI, USA) prior to ovariectomy or sham surgeries, and re-measured at 12 weeks postoperatively [20].

Surgical procedures

One day before surgery, rabbits were fasted overnight and intramuscularly injected with cefazolin (33mg/kg). They were sedated and anesthetized intraperitoneally with ketamine (100mg/kg) and xylazine (10mg/kg) on the day of surgery. To avoid contamination in the surgical field, an electric shaver was used to shave the proximal medial region of the tibia, and washed with povidone-iodine solution. Rabbits were injected with articaine (1:100000 epinephrine). Then, the skin was incised with a scalpel, and the soft tissues were separated for exposing the bone. A hole was drilled on the flat surface of the tibia using a 2.5-mm diameter dental split drill accompanying the irrigation of sterile saline. The implant was inserted manually into the drilled hole with a 15N torque 0.5mm above the upper tibial cortex. The rabbits in three groups were all implanted with Matrigel and were implanted over the entire implant. SHAM group rabbits were implanted with Matrigel containing 5uL AAV empty vector, while OVX rabbits were implanted with Matrigel containing 5uL AAV empty vector or adeno-associated virus vector overexpressing rabbit Sema3A, respectively. The concentration of AAV empty vector and AAV vector overexpression was approximately 10×10^9 vg/ml. After implantation, the surgical site was sutured in layers (Supplemental Figure.2). Penicillin was administered intramuscularly for postoperative three days to prevent infection. On the 4th and 12th week of post-implantation, two rabbits per group were euthanized with an overdose

intravenous injection of 20% trichloroacetaldehyde hydrate (Sinopharm, Shanghai, China) solution. The tibia sample was collected and immediately immersed in a 4% neutral formalin solution for 48h.

Immunocytochemistry

Rabbit bone samples were decalcified in EDTA at RT for 21 days, and the decalcification solution was replaced every other day. Subsequently, bone samples were dehydrated, paraffin embedded and heated at 37°C for 2 h. After dewaxing in xylene and rehydrating in gradient concentrations of ethanol, sections were subjected to 10-min incubation in 3% H_2O_2, and 20-min boiling in citric acid buffer (pH=6.0). They were then incubated with 10% bovine serum albumin, and immunoreacted with rabbit anti-RUNX2 (Cell Signaling Technology, Inc., Danvers, MA, USA). After washing, sections were immunoreacted with goat anti-rabbit secondary antibody (Cell Signaling Technology, Inc., Danvers, MA, USA) at RT for 1 h. Tissue sections were dyed in 3,3′-diaminobenzidine (DAB), and counterstained with hematoxylin, dehydrated, cleaned, and fixed. These sections were stained by hematoxylin and eosin-dyed to confirm microscopic characteristics.

Radiographic examination

All bone mass samples containing the implants were scanned by micro-computed tomography (SkyScan, Kontich, Belgium). A high-resolution scanner (image pixel size =27.45μm, source voltage = 90kV, source current = 100μA, and exposure time = 1500ms) and 3D reconstruction software (SkyScan, Kontich, Belgium) were used to generate 3D models and obtain images within the regions of interest. Reconstructed images were segmented, registered, and quantized. A total of three variables in two regions of interest along the length of the implant were analyzed. Meanwhile, the equivalent peri-implant volume-of-interest (VOI) per sample was calculated to estimate the surrounding bone of the implant. Three variables were included, the 3D bone-to-implant contact ratio, a 500-μm fixed VOI zone surrounding the implant surface and used to analyze the bone volume: tissue volume (BV/TV) of newly formed bone on the implant surface and reconstructed 3D images of surrounding bones of the implant at 500 μm from the implant surface in a volume rendering function.

Histological examination

Bone samples were fixed in formalin for 48 h and then gently washed with slow running water for 24 h. Following dehydration with gradient ethanol and vitrification with dimethyl benzene, samples containing implants were induced in a mixture of absolute alcohol and Technovit 7200 resin solution (Heraeus Kulzer, Germany) (3:7) for 2 days, and then soaked in a mixture of absolute alcohol and Technovit 7200 resin solution (1:1) for 2 days. Later, samples were soaked in Technovit 7200 resin solution for 7 days and a fresh one for 3 days, which were embedded and polymerized with a light-curing machine. The implanted samples were longitudinally sliced in 200 μm thickness using an automatic slicer (EXAKT, 300CP, Germany), and polished using a 320, 800, 1200, and 400 mesh Buehler (EXAKT, 400CS, Germany) to the thickness of 25 μm. Hard tissue sections were stained with methylene blue acid fuchsin staining solution to distinguish osteoblasts, mineralized bones, and osteoid tissues. Bone morphology was observed and implant osseointegration rate was calculated by experienced researchers using OsteoMeasurexp (version 1.01).

Biomechanical test

The tibiae with implants were tested using a commercial material testing system (Instron 4302; Instron, Norwood, MA) immediately after harvest. The two ends of the implant were exposed about 2mm. A custom mold made of self-curing plastic was prepared for each sample. Pressure was applied from the distal end of the implant at a speed of 1mm/min, and calculated the maximum push-out force (N), stiffness (N/mm), and toughness (N.mm) based on the displacement-force curve.

Statistical analyses

SPSS 18.0 (SPSS, Inc., Chicago, IL, USA) and GraphPad Prism software (GraphPad Software, Inc., La Jolla, CA, USA) were used for statistical processing. All data were expressed as mean± standard deviation (SD). The Student's t-test and one-way analysis of variance (ANOVA) were conducted to compare differences between two and multiple groups, respectively. A significant difference was set at $p<0.05$ ($^*P<0.05$, $^{**}P<0.01$, and $^{***}P<0.001$).

Results

Overexpression of Sema3A promotes osteogenic differentiation

To confirm the role of Sema3A in osteogenesis, HBMSCs were stimulated to osteogenesis, followed by examination of osteogenesis, ALP activity, and mineralization matrix formation. QRT-PCR and Western blotting data both showed that transfection of Sema3A significantly altered osteogenesis markers ALP, OCN, and OPN (Fig. 1a, b). Besides,
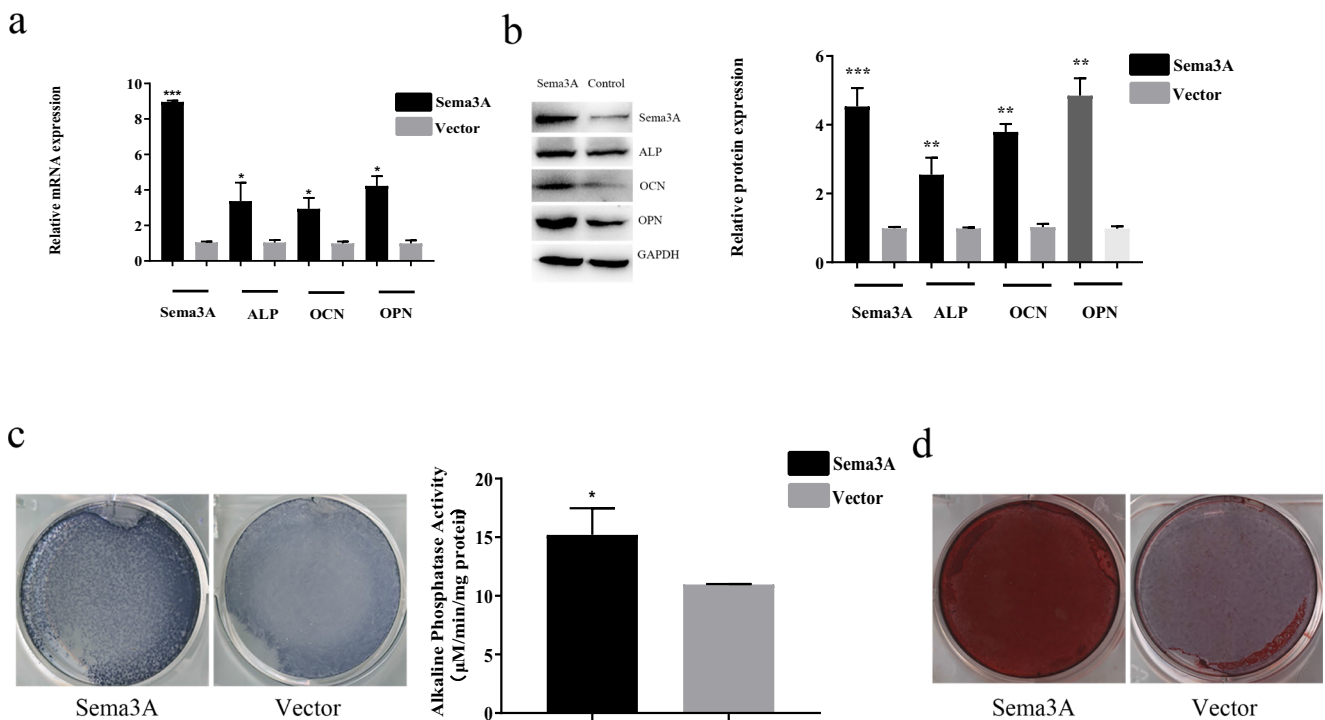
Fig. 1 The effect of Sema3A on osteogenesis. **a**, **b** qRT-PCR and Western blotting analyses examined the transfection efficacy of Sema3A overexpression in HBMSCs. **c** ALP activity measured after 10-day osteogenic induction using the ALP assay kit. **d** Mineralized matrix formation measured after 14-day osteogenic induction using Alizarin Red S staining. $^*p < 0.05$, $^{**}p < 0.01$

transfection of Sema3A remarkably improved osteogenic compatibility in HBMSCs, manifesting as enhanced mineralization and ALP activity (Fig. 1c, d).

Sema3A modulates the activity of the NF-kappa B signaling

Recent studies have shown the ability of Sema3A in mediating the NF-kappa B signaling. Here, to explore the association between Sema3A and NF-kappa B signaling in HBMSCs cells, the role of canonical NF-kappa B signaling in regulating Sema3A overexpression or knockdown-mediated osteogenesis by HBMSCs was elucidated. The transfection efficiency of Sema3A siRNAs was examined by Western blotting (Supplemental Figure 3). The mRNA levels of p65 and IκBα were examined by qRT-PCR (Fig. 2a, b). Compared with the control group, NF-kappa B signaling pathway activity was inhibited in overexpression of Sema3A. Meanwhile, knockdown of Sema3A activated the NF-kappa B signaling (Fig. 2a, b). Furthermore, we examined the protein expression of overexpression or knockdown of Sema3A; these results were consistent with previous studies (Fig. 2c, d).

Sema3A is downregulated in rabbits of the OVX group

Rabbit ovaries were removed following standard procedures (Supplemental Figure.1). The mean BMD (g/cm^2) of the lumbar spines (L3–L6) was determined before and after OVX or sham operations. At postoperative 12 weeks, a lower mean BMD in the OVX group compared with that of the SHAM group confirmed the successful establishment of the osteoporosis model in rabbits (Table 1). BV/TV of the cancellous bone was listed in Table 2. Immunohistochemical results also confirmed our verification (Fig. 3a, b). Micro-CT images of the proximal femur were captured in rabbits (Fig. 3c). Compared with sham rabbits, we observed evident cortical porosity, decreased cancellous bone density, magnophyric trabeculae of cancellous bones, low-density changes of honeycomb, or irregular small pieces and thinning cortical bones in representative reconstructed images of the OVX group. In addition, a lower mRNA level of Sema3A was detected in the OVX group than controls (Fig. 3d).

Sema3A promotes osseointegration of titanium implants

Bone quality of the proximal tibia of rabbits around implants in each group at 4 and 12 weeks after implantation was assessed by micro-CT reconstructed 3D models (Fig. 4). Histological analyses demonstrated that Sema3A around the implants pronouncedly protected the bone density and osseointegration of implants. Besides, the surface bone mass and the bone-to-implant contact ratio of the OVX group were remarkably lower than the SHAM group. At
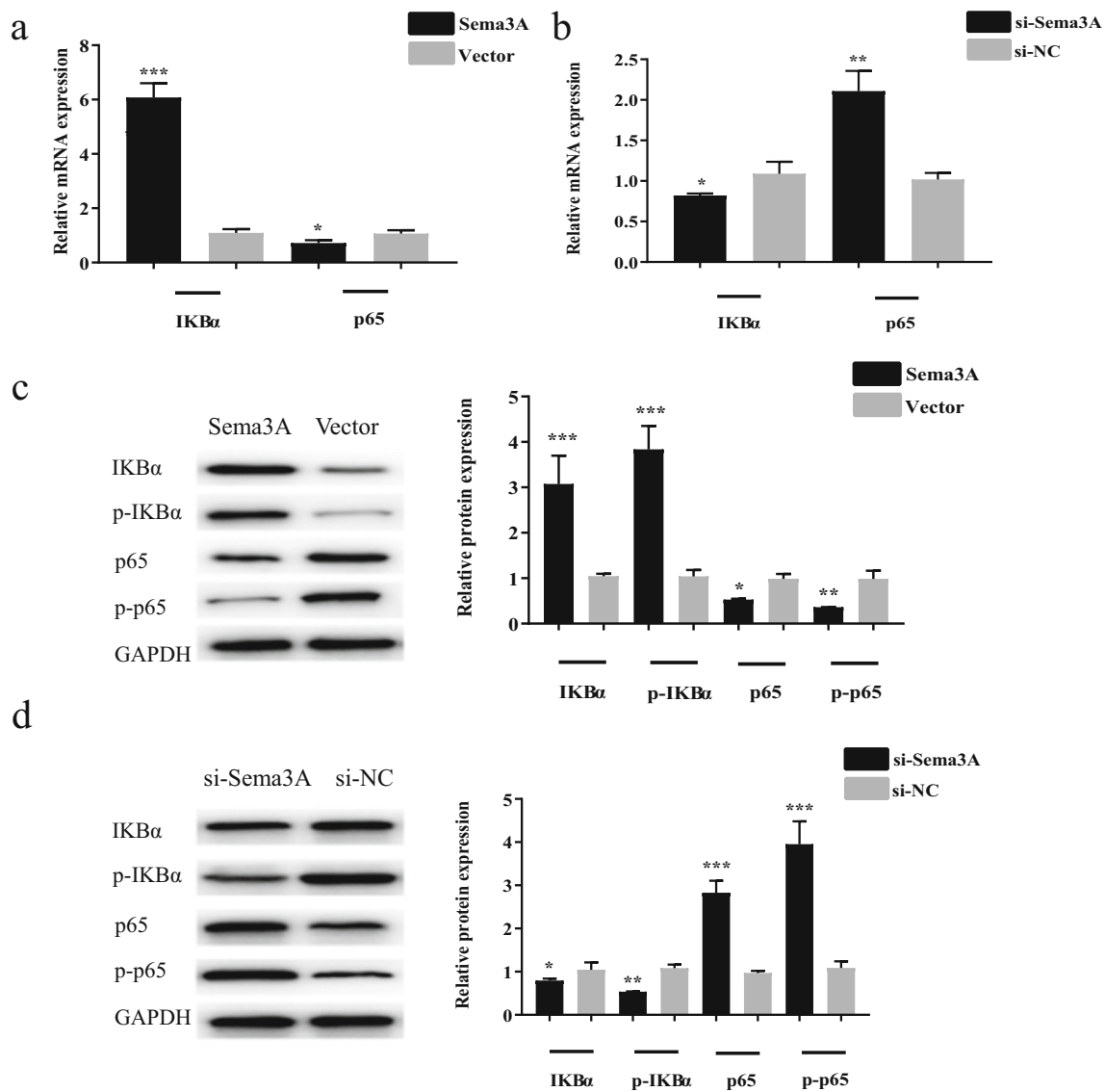
Fig. 2 Sema3A regulated the NF-kappa B signaling in HBMSCs. The mRNA levels of IκBα and p65 in HBMSCs overexpressing Sema3A (**a**) or silencing Sema3A (**b**). The protein levels of IκBα, p-IκBα, p65, and p-p65 in HBMSCs overexpressing Sema3A (**c**) or silencing Sema3A (**d**). $^*p < 0.05$, $^{**}p < 0.01$, $^{***}p < 0.001$

Table 1 Quantitative results of biomechanical test of implant fixation 4 and 12 weeks after implant insertion, presented as the maximal push-out force, stiffness, and toughness

	SHAM	OVX	OVX+Sema3A
4 weeks			
Maximal push-out force	78.2±4.5**	40.6±3.1	42.5±4.9
Stiffness	238.8±23.1**	169.8±20.2	167.4±15.3
Toughness	49.3±3.8**	22.3±1.4	23.4±3.1
12 weeks			
Maximal push-out force	283.9±20.2**	100.4±15.8	190.2±18.3*
Stiffness	495.2±49.2**	275.4±30.2	383.9±27.3*
Toughness	174.3±18.8**	89.3±7.4	146.3±6.3*

Data were expressed as mean ± standard deviation (SD). $^*p < 0.05$, $^{**}p < 0.01$ vs. OVX (Student's t-test)

12 weeks, the contact between the bone and the implant was satisfactory in both experimental groups, especially in the OVX+Sema3A group. A representative image of the methylene blue acid fuchsin–stained section was shown in Fig. 5a and Supplemental Figure 4. In comparison with rabbits of the SHAM group, Sema3A significantly increased bone mass around the implant (Fig. 5b). Biomechanical results showed that Sema3A had a protective effect on implant fixation in ovariectomized rabbits. Compared with the SHAM group, the values of the other two groups were significantly lower. And there was no significant difference in all parameters at 4 weeks between the OVX group and OVX+Sema3A group. However, compared with the OVX group, the maximum

Table 2 Bone mineral density (BMD)(g/cm^2) before operation and at 12 weeks postoperatively

Time	SHAM	OVX
Pre-operation	0.324±0.017	0.321±0.019
Post-operation	0.329±0.021	0.224±0.021*
Decrease(%)	1.45±1.15	30.36±2.42

*$P<0.01$

push-out force increased by 89.4%, the stiffness increased by 39.4%, and the toughness increased by 63.8% in the OVX+Sema3A group at 12 weeks (Table 3).

Discussion

Osteoporosis has been a public health problem of considerable concern, with the aging population [21]. Osteoporosis is a common metabolic bone disease featured by decreased bone mass and quality, and disruption of bone microarchitecture, resulting in compromised bone strength and fracture risks [22]. In addition, osteoporosis also influences dental implantation [23]. Previous studies have shown that osteoporosis reduces the stability and success rate of implant restoration [24]. How to improve the osseointegration of implants in osteoporosis patients is a challenge in the medical field. With the recent advancement and development of medical technologies, implant restoration has become more common in clinical practice, which replaces traditional removable and fixed partial dentures [25]. As a result, implants have been widely used in replacing missing teeth. Besides, implants are also widely used in the plastic repair of defective maxilla and mandible. However, osteoporosis greatly limits the clinical application of implants because osteoporosis-caused low bone density significantly influences osseointegration [26].

In recent years, several concerns have been raised on the surface modification of titanium alloy, which illustrates that the surface modification technologies play a significant role in improving the surface properties of the implant [27, 28]. Some special treatments, including coating or activation of the implant surface, can promote osseointegration of the implant. Bone tissue engineering can be enhanced by the Sema3A gene to promote local osteogenic activity through biological self-regulation, thereby eliminating the possible adverse effects of heterogeneous or xenogeneic materials. Sema3A is identified to be important in bone metabolism, which is capable of reducing the calcium absorption capacity of osteoclasts, and promoting the formation of osteoblasts [13]. After Sema3A binds to Nrp1, RANKL-induced osteoclast differentiation is suppressed. Abundant classic pathways can be activated by almost all stimuli that affect the NF-kappa B signaling, including the major osteoclast factor RANKL, TNFα, and other inflammatory mediators. The IKK complex is the fundamental key regulator of the NF-kappa B signaling pathway, including IKKα and IKKβ. It targets IκBα and induces its degradation, thus activating the classic p65 signaling pathway. Since IκBα is one of the earliest transcription target of the NF-kappa B signaling pathway, a transient activation, as a result, is emerged by an effective negative feedback loop. Sema3A also regulates bone remodeling through sensory nerves. Distinct from other proteins, Sema3A significantly inhibits the activity of osteoclasts, while promoting that of osteoblasts. It produces a stronger osteogenic effect and osteolysis in osteoporosis patients. Sema3A may, therefore, be a promising agent for improving bone health in elderly patients. Current research on biotechnology development intends to improve biological sources, aiming to improve the function of human tissues and organs.

Hayashi M et al. determined the therapeutic potential of Sema3A in a cortical bone defect model in mice [13]. Sema3A significantly accelerates bone regeneration, manifesting as increased volume of regenerated bone in the mouse cortex, recovered osteoblast parameters, and decreased osteoclast parameters around the injured area [15]. Sema3A treatment, in conclusion, rescues bone loss in ovariectomized mice. Permuy et al. and Calciolari et al. reported that OVX rabbits and rats are generally used osteoporosis models because of convenient procedures and high replicability [29, 30]. An osteoporosis model established by OVX is usually used to the research on secondary osteoporosis. However, primary osteoporosis after menopause or aging cannot be simulated. A previous study demonstrated that at post-ovariectomy, potential influences on osteoporosis-induced bone and mineral metabolism are time-dependent [31]. In the present study, bone mass of OVX-operated rabbits was significantly reduced at postoperative 12 weeks, indicating the successful establishment of the in vivo osteoporosis model. An ovariectomized rabbit presents decreased mineral density and BMD in a short period, which are similar to post-menopausal conditions. In addition, ovariectomized rabbits develop a relatively rapid bone renewal and bone remodeling process.

Fig. 3 The expression of Sema3A was low in osteoporosis group. Representative images for **a** H&E staining and **b** immunohistochemistry of RUNX2, and quantification of the number of positive cells. **c** The model of the micro-CT analysis. **d** Differences of Sema3A and osteogenic-related genes between OVX group and SHAM group. Data were presented as mean ± SEM. Original magnification = 100×. $^*p < 0.05$, $^{**}p < 0.01$
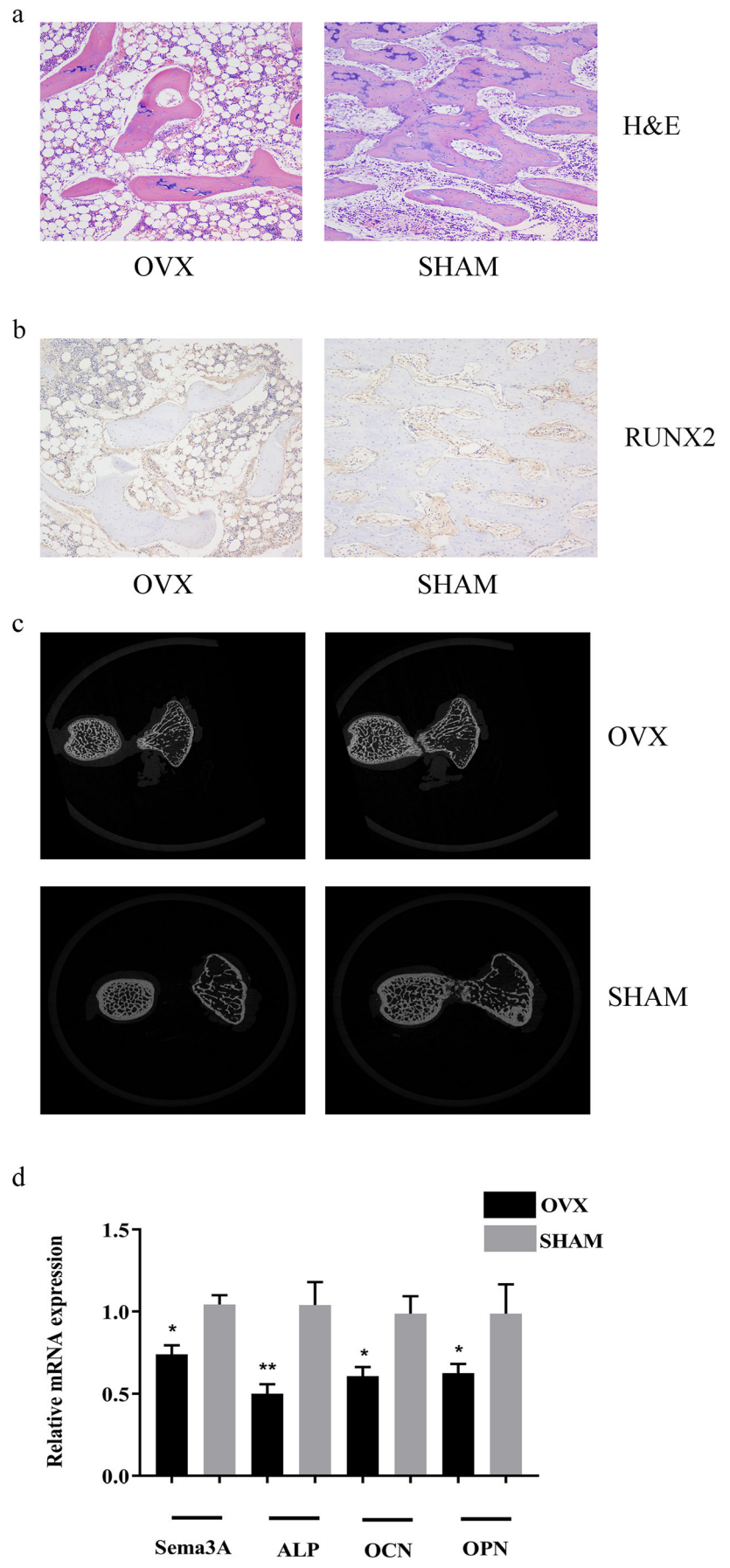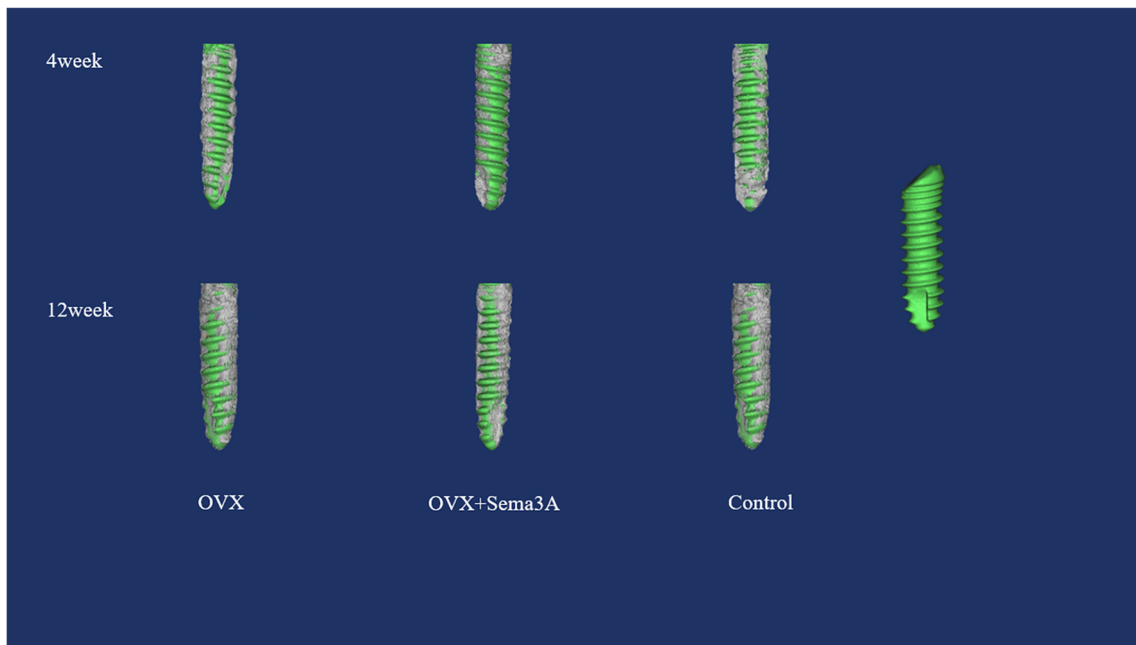
Fig. 4 Representative 3D reconstructed images of peri-implant bone at a distance of 500μm from the outer surface of the implant at 4 and 12 weeks after implantation. The gray color represented bone tissues, while the green color represented the implant

Fig. 5 Histology and histomorphometric analysis. **a** The hard tissue slices were stained with methylene blue acid fuchsin of post-implantation bone at 4 and 12 weeks. **b** The statistical figure of BIC using OsteoMeasurexp software analysis with implants from OVX, OVX+Sema3A, and SHAM groups at 4 and 12 weeks. $^*p < 0.05$, $^{**}p < 0.01$
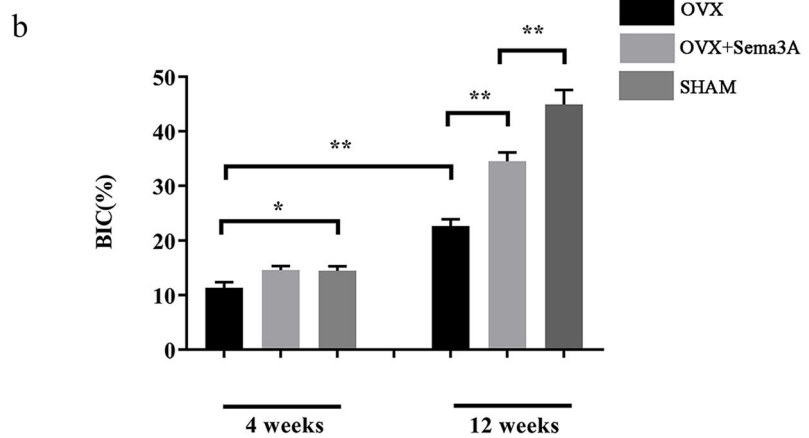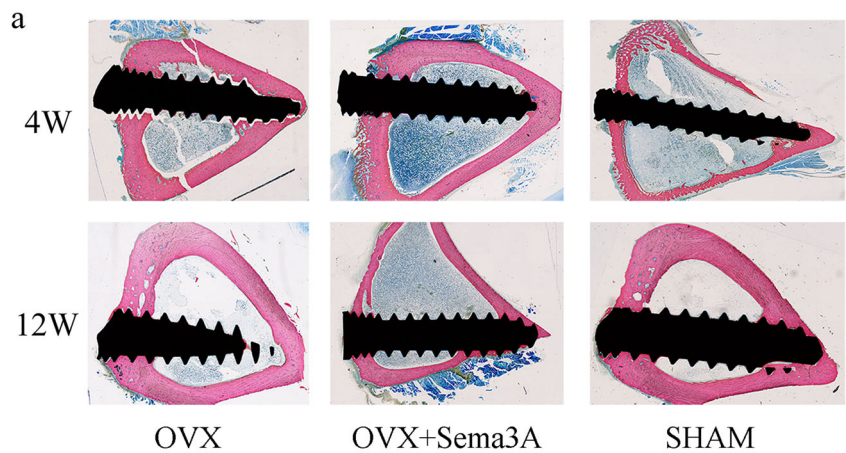
Table 3 The data of BV/TV of peri-implant bone at 4 weeks and 12 weeks post-implantation

Time	OVX	OVX+Sema3A	SHAM
4w	26.89%±2.19%	28.11%±3.43%	28.23%±3.45%
12w	28.44%±4.21%	32.43%±2.94%*	34.9%±2.12%*

Data were expressed as mean ± standard deviation (SD). $^*p < 0.05$ vs. OVX (Student's t-test)

Here, Sema3A was used to the treatment of abnormal bone metabolism. In vitro experiments revealed that overexpression of Sema3A in HBMSCs had no side effects and significantly upregulated osteoblast-related genes, and accelerated calcium deposition. Sema3A inhibited the osteoclast formation of in vitro cultured HBMSCs and promoted the formation of osteoblasts via NF-kappa B signaling. Therefore, Sema3A can exert an effective bone protection by simultaneously suppressing bone resorption and promoting bone formation.

In the present study, the implant was embedded in the tibial metaphysis as previously reported [32]. Sema3A adeno-associated virus vector was injected around the implant and the expression level of Sema3A around the peri-implant was significantly upregulated. Micro-CT, histological, and histomorphological analysis showed that Sema3A remarkably increased newly formed surrounding bones of the implant and the trabecular bone. Such a favorable microstructure was conductive to the fixation of implants and the formation of new bones around the implant of osteoporosis rabbits. Here, we found that there was no significant difference in OVX and OVX+Sema3A at 4 weeks. It may be that AAV vector overexpressing Sema3A affects the osteogenic differentiation of bone marrow mesenchymal stem cells and it still takes some time. And we observed a significant difference in 12 weeks. Although compared with the normal group, the osseointegration ability of the OVX+Sema3A group was still not satisfactory, but compared with OVX, the osseointegration ability was significantly improved. Hence, Sema3A is conductive to new bone formation or bone resorption decline, or both. However, further research is required to reveal the mechanism of Sema3A on implant osseointegration. Although our statistical error is very small (a small part of the extrapolation error bar), the results are relatively accurate. However, the small number of experimental animals may affect the accuracy of the results. Therefore, we will expand the number of samples and extend the experiment period in further experiments to obtain more convincing results.

In summary, our research demonstrated that Sema3A significantly increased the BMD of peri-implant cancellous bone and had a positive effect on promoting early osseointegration of titanium implants in osteoporotic rabbits. It is concluded that local application of Sema3A can improve the osteogenic ability of bone marrow stem cells and promotes osseointegration during osteoporosis. Therefore, gene therapy of Sema3A is a promising approach to accelerate implant fixation in osteoporosis patients, the elderly and climacteric women.

Abbreviations HBMSCs, Human bone mesenchymal stem cells; OVX, Ovariectomy

Author contributions An Song and Junbo Zhou conceived the study design and drafted the article together. An Song, Feng Jiang, Yi Wang, and Yang Zheng performed the experiments and analyzed the data. Ming Wang and Yanhui Wu managed the biobank, Xiaomeng Song and Wei Zhang sought approval from the ethics committee, and provided funding. All authors discussed, revised, and approved the final manuscript.

Declarations

Conflict of interest The authors declare that they have no conflicts of interest.

Ethical approval This study was approved by the Animal Care Committee of Nanjing First Hospital, Nanjing Medical University (IACUC Approval No. SYXK20160006). All animal procedures were in accordance with the Guidelines of International Standards on the Animal Ethical and Welfare Committee (AEWC), and the ARRIVE guideline for the care and use of laboratory animals released by National Institutes of Health (NIH Publications No. 8023, revised in 1978).

References

1. Rachmiel A, Shilo D (2015) The use of distraction osteogenesis in oral and maxillofacial surgery. Ann Maxillofac Surg 5:146–147. https://doi.org/10.4103/2231-0746.175777

2. Li J, Yin X, Huang L, Mouraret S, Brunski JB, Cordova L, Salmon B, Helms JA (2017) Relationships among bone quality, implant osseointegration, and Wnt signaling. J Dent Res 96:822–831. https://doi.org/10.1177/0022034517700131

3. Fang CH, Lin YW, Lin FH, Sun JS, Chao YH, Lin HY, Chang ZC (2019) Biomimetic synthesis of nanocrystalline hydroxyapatite composites: therapeutic potential and effects on bone regeneration. Int J Mol Sci 20. https://doi.org/10.3390/ijms20236002

4. Tavangar A, Tan B, Venkatakrishnan K (2011) Synthesis of three-dimensional calcium carbonate nanofibrous structure from eggshell using femtosecond laser ablation. J Nanobiotechnology 9:1. https://doi.org/10.1186/1477-3155-9-1

5. Suzuki T, Nakamura Y, Kato H (2018) Vitamin D and calcium addition during denosumab therapy over a period of four years significantly improves lumbar bone mineral density in Japanese osteoporosis patients. Nutrients 10. https://doi.org/10.3390/nu10030272

6. Chesi A, Wagley Y, Johnson ME, Manduchi E, Su C, Lu S, Leonard ME, Hodge KM, Pippin JA, Hankenson KD, Wells AD, Grant SFA (2019) Genome-scale capture C promoter interactions implicate effector genes at GWAS loci for bone mineral density. Nat Commun 10:1260. https://doi.org/10.1038/s41467-019-09302-x

7. Doornewaard R, Glibert M, Matthys C, Vervaeke S, Bronkhorst E, de Bruyn H (2019) Improvement of quality of life with implant-supported mandibular overdentures and the effect of implant type and surgical procedure on bone and soft tissue stability: a three-year prospective split-mouth trial. J Clin Med 8:8. https://doi.org/10.3390/jcm8060773

8. Khandaker M, Riahinezhad S, Williams WR, Wolf R (2017) Microgroove and collagen-poly(epsilon-caprolactone) nanofiber mesh coating improves the mechanical stability and osseointegration of titanium implants. Nanomaterials (Basel) 7. https://doi.org/10.3390/nano7060145

9. De La Vega RE, De Padilla CL, Trujillo M, Quirk N, Porter RM, Evans CH, Ferreira E (2018) Contribution of implanted, genetically modified muscle progenitor cells expressing BMP-2 to new bone formation in a rat osseous defect. Mol Ther 26:208–218. https://doi.org/10.1016/j.ymthe.2017.10.001

10. Sample SJ, Behan M, Smith L, Oldenhoff WE, Markel MD, Kalscheur VL, Hao Z, Miletic V, Muir P (2008) Functional adaptation to loading of a single bone is neuronally regulated and involves multiple bones. J Bone Miner Res 23:1372–1381. https://doi.org/10.1359/jbmr.080407

11. Lin D, Chai Y, Ma Y, Duan B, Yuan Y, Liu C (2019) Rapid initiation of guided bone regeneration driven by spatiotemporal delivery of IL-8 and BMP-2 from hierarchical MBG-based scaffold. Biomaterials 196:122–137. https://doi.org/10.1016/j.biomaterials.2017.11.011

12. Kaneko S, Iwanami A, Nakamura M, Kishino A, Kikuchi K, Shibata S, Okano HJ, Ikegami T, Moriya A, Konishi O, Nakayama C, Kumagai K, Kimura T, Sato Y, Goshima Y, Taniguchi M, Ito M, He Z, Toyama Y, Okano H (2006) A selective Sema3A inhibitor enhances regenerative responses and functional recovery of the injured spinal cord. Nat Med 12:1380–1389. https://doi.org/10.1038/nm1505

13. Hayashi M, Nakashima T, Taniguchi M, Kodama T, Kumanogoh A, Takayanagi H (2012) Osteoprotection by semaphorin 3A. Nature 485:69–74. https://doi.org/10.1038/nature11000

14. Casazza A, Laoui D, Wenes M, Rizzolio S, Bassani N, Mambretti M, Deschoemaeker S, Van Ginderachter JA, Tamagnone L, Mazzone M (2013) Impeding macrophage entry into hypoxic tumor areas by Sema3A/Nrp1 signaling blockade inhibits angiogenesis and restores antitumor immunity. Cancer Cell 24:695–709. https://doi.org/10.1016/j.ccr.2013.11.007

15. Giacobini P, Parkash J, Campagne C, Messina A, Casoni F, Vanacker C, Langlet F, Hobo B, Cagnoni G, Gallet S, Hanchate NK, Mazur D, Taniguchi M, Mazzone M, Verhaagen J, Ciofi P, Bouret SG, Tamagnone L, Prevot V (2014) Brain endothelial cells control fertility through ovarian-steroid-dependent release of semaphorin 3A. PLoS Biol 12:e1001808. https://doi.org/10.1371/journal.pbio.1001808

16. Mediero A, Wilder T, Shah L, Cronstein BN (2018) Adenosine A2A receptor (A2AR) stimulation modulates expression of semaphorins 4D and 3A, regulators of bone homeostasis. FASEB J 32:3487–3501. https://doi.org/10.1096/fj.201700217R

17. Novack DV (2011) Role of NF-kappaB in the skeleton. Cell Res 21:169–182. https://doi.org/10.1038/cr.2010.159

18. Le Henaff C, Mansouri R, Modrowski D, Zarka M, Geoffroy V, Marty C, Tarantino N, Laplantine E, Marie PJ (2015) Increased NF-kappaB activity and decreased Wnt/beta-catenin signaling mediate reduced osteoblast differentiation and function in deltaF508 cystic fibrosis transmembrane conductance regulator (CFTR) mice. J Biol Chem 290:18009–18017. https://doi.org/10.1074/jbc.M115.646208

19. Bian Y, Du Y, Wang R, Chen N, Du X, Wang Y, Yuan H (2019) A comparative study of HAMSCs/HBMSCs transwell and mixed co-culture systems. IUBMB Life 71:1048–1055. https://doi.org/10.1002/iub.2074

20. Wen B, Zhu F, Li Z, Zhang P, Lin X, Dard M (2014) The osseointegration behavior of titanium-zirconium implants in ovariectomized rabbits. Clin Oral Implants Res 25:819–825. https://doi.org/10.1111/clr.12141

21. Khosla S, Amin S, Orwoll E (2008) Osteoporosis in men. Endocr Rev 29:441–464. https://doi.org/10.1210/er.2008-0002

22. Huang Y, Chen N, Miao D (2017) Effect and mechanism of pyrroloquinoline quinone on anti-osteoporosis in Bmi-1 knockout mice-anti-oxidant effect of pyrroloquinoline quinone. Am J Transl Res 9:4361–4374

23. Madrid C, Sanz M (2009) What impact do systemically administrated bisphosphonates have on oral implant therapy? A systematic review. Clin Oral Implants Res 20(Suppl 4):87–95. https://doi.org/10.1111/j.1600-0501.2009.01772.x

24. Yoshioka Y, Yamachika E, Nakanishi M, Ninomiya T, Akashi S, Kondo S, Moritani N, Kobayashi Y, Fujii T, Iida S (2019) Intermittent parathyroid hormone 1-34 induces oxidation and deterioration of mineral and collagen quality in newly formed mandibular bone. Sci Rep 9:8041. https://doi.org/10.1038/s41598-019-44389-8

25. Nogawa T, Takayama Y, Ishida K, Yokoyama A (2016) Comparison of treatment outcomes in partially edentulous patients with implant-supported fixed prostheses and removable partial dentures. Int J Oral Maxillofac Implants 31:1376–1383. https://doi.org/10.11607/jomi.4605

26. Xu B, Zhang J, Brewer E, Tu Q, Yu L, Tang J, Krebsbach P, Wieland M, Chen J (2009) Osterix enhances BMSC-associated osseointegration of implants. J Dent Res 88:1003–1007. https://doi.org/10.1177/0022034509346928

27. Das S, Dholam K, Gurav S, Bendale K, Ingle A, Mohanty B, Chaudhari P, Bellare JR (2019) Accentuated osseointegration in osteogenic nanofibrous coated titanium implants. Sci Rep 9: 17638. https://doi.org/10.1038/s41598-019-53884-x

28. Wang Q, Zhou P, Liu S, Attarilar S, Ma RL, Zhong Y, Wang L (2020) Multi-Scale Surface treatments of titanium implants for rapid osseointegration: a review. Nanomaterials (Basel) 10. https://doi.org/10.3390/nano10061244

29. Permuy M, Lopez-Pena M, Munoz F, Gonzalez-Cantalapiedra A (2019) Rabbit as model for osteoporosis research. J Bone Miner Metab 37:573–583. https://doi.org/10.1007/s00774-019-01007-x

30. Calciolari E, Donos N, Mardas N (2017) Osteoporotic animal models of bone healing: advantages and pitfalls. J Investig Surg 30:342–350. https://doi.org/10.1080/08941939.2016.1241840

31. Jiang Z, Li Z, Zhang W, Yang Y, Han B, Liu W, Peng Y (2018) Dietary natural N-Acetyl-d-glucosamine prevents bone loss in ovariectomized rat model of postmenopausal osteoporosis. Molecules 23:23. https://doi.org/10.3390/molecules23092302

32. Suh JY, Jeung OC, Choi BJ, Park JW (2007) Effects of a novel calcium titanate coating on the osseointegration of blasted endosseous implants in rabbit tibiae. Clin Oral Implants Res 18: 362–369. https://doi.org/10.1111/j.1600-0501.2006.01323.x